
EFDA–JET–PR(02)28

J. Rapp, P. Monier-Garbet, P. Andrew, P. Dumortier, T. Eich, W. Fundamenski,
M. von Hellermann, J. Hogan, L.C. Ingesson, S. Jachmich, H.R. Koslowski,
A. Loarte, G. Maddison, G.F. Matthews, D.C. McDonald, A. Messiaen,
J. Ongena, V. Parail, V. Philipps, G. Saibene, R. Sartori and B. Unterberg

Reduction of Divertor Heat Load in JET ELMy H-modes using Impurity Seeding Techniques

Reduction of Divertor Heat Load in JET ELMy H-modes using Impurity Seeding Techniques

J. Rapp^{1,9}, P. Monier-Garbet², P. Andrew³, P. Dumortier⁴, T. Eich⁵, W. Fundamenski³,
M. von Hellermann⁶, J. Hogan⁷, L.C. Ingesson⁶, S. Jachmich³, H.R. Koslowski¹,
A. Loarte⁸, G. Maddison³, G.F. Matthews³, D.C. McDonald³, A. Messiaen⁴,
J. Ongena⁴, V. Parail³, V. Philipps¹, G. Saibene⁸, R. Sartori⁸, B. Unterberg¹
and contributors to the EFDA-JET workprogramme*

¹*Institut für Plasmaphysik, Forschungszentrum Jülich GmbH, EURATOM Association, TEC, Jülich, Germany*

²*Association EURATOM-CEA sur la Fusion Contrôlée, Cadarache, Saint-Paul-lez-Durance, France*

³*EURATOM-UKAEA/Fusion Association, Culham Science Centre, Abingdon, OXON, UK*

⁴*LPP-ERM/KMS, EURATOM-Belgian State Association, TEC, Brussels, Belgium*

⁵*Max-Planck Institut für Plasmaphysik, EURATOM Association, Garching, Germany*

⁶*FOM Instituut for Plasmafysica Rijnhuizen, Association EURATOM-FOM, TEC, Nieuwegein,
The Netherlands*

⁷*Oak Ridge National Laboratory, USA*

⁸*EFDA, CSU-Garching, Garching, Germany*

⁹*EFDA-JET, CSU-Culham, Culham Science Center, Abingdon, OXON, UK*

* See annex of J. Pamela et al, "Overview of Recent JET Results and Future Perspectives",
Fusion Energy 2000 (Proc. 18th Int. Conf. Sorrento, 2000), IAEA, Vienna (2001).

“This document is intended for publication in the open literature. It is made available on the understanding that it may not be further circulated and extracts or references may not be published prior to publication of the original when applicable, or without the consent of the Publications Officer, EFDA, Culham Science Centre, Abingdon, Oxon, OX14 3DB, UK.”

“Enquiries about Copyright and reproduction should be addressed to the Publications Officer, EFDA, Culham Science Centre, Abingdon, Oxon, OX14 3DB, UK.”

ABSTRACT.

The investigation of methods for a reduction of divertor heat loads in order to increase the lifetime of divertor tiles in future fusion reactors is the main objective of this paper. Special emphasis is given to the reduction of transient heat loads due to Edge Localised Modes (ELMs). Two methods are compared: Argon seeded type-I ELMy H-modes and Nitrogen seeded type-III ELMy H-modes. In both scenarios the impurity seeding leads to a reduction of the pedestal energy and hence a reduction of the energy released by the ELM. This consequentially reduces the power load to the divertor targets. At high radiative power fractions in type-III ELMy H-modes part of that released ELM energy (25kJ) is dissipated by radiation in the Scrape-Off-Layer (SOL). Modelling of the ELM mitigation supports the experimental findings. Both scenarios might be compatible with an integrated ITER scenario, with respect to acceptable divertor lifetime and acceptable confinement.

1. INTRODUCTION

One of the most severe problems for fusion reactors is the power load to the divertor target plates. Technically only steady state power loads of less than 10 MW/m² are acceptable with margin. In order to reduce the power load in the divertor to those values radiation cooling by seeding of impurities is essential, especially in future devices with tungsten divertors where radiation due to intrinsic impurities is minimal. Furthermore transient heat loads due to Edge Localised Modes (ELMs) have to be reduced to values below 40MJ m⁻² s^{1/2} (for a tungsten target). Presently unseeded type-I ELMy H-modes seem to be problematic. Alternative operating scenarios with tolerable transient heat loads have to be developed. One of the potential alternative scenarios is the ELMy H-mode with impurity seeding. Other potential solutions are the type-II ELMy regime and ELM mitigation by frequent pellet injection, which are not discussed in this paper. The present paper summarises the work aimed at the reduction of the heat load to the target plates, both during, and inbetween ELMs, using the radiation of a purposely injected impurity. Two scenarios are described, type-I ELMy H-modes with impurity seeding and type-III ELMy H-modes with impurity seeding.

2. RADIATIVE TYPE-III ELMY H-MODES

In the first scenario described Nitrogen is seeded in type-III ELMy H-modes up to radiative power fractions of 90%. In low triangularity configurations [1] this regime leads to a partially detached H-mode at 85% of the Greenwald density, confinement enhancement factors of $H_{98(Y,2)} \approx 0.7-0.85$ with a normalised plasma pressure of β_N 1.3-1.4.

The steady state heat flux density is reduced to less than 1MW/m² and electron temperatures in the divertor of less than 10eV even during ELM peaks are feasible. There is an indication of radiative dissipation of ELM energy at high radiative power fractions (90%), which reduces the ELM power load by a factor of 2 and leads to transient power loads due to ELMs of less than 5MW/m² at the outer divertor target plate [1]. At high radiative power fractions above $\approx 70\%$ the ELM loss from the plasma is as lower than 25kJ [1]. For these low ELM energies the divertor plasma stays attached even during

the ELM energy pulse. If the radiative power fraction is further increased up to 90%, the electron temperature in front of the outer divertor, as measured by Langmuir Probes, does not increase to more than 10eV during the ELM event. This is consistent with the radiation characteristic of Nitrogen. The cooling rate of Nitrogen drops significantly in the temperature range from 10 - 30eV. Thus Nitrogen radiates most efficiently in the temperature range of 10 eV. As a result radiative dissipation of ELM energy is observed at radiative power fractions above 80% (see figure 1). Radiative dissipation in this sense means, that target heat flux is stronger reduced than the energy loss due to ELMs from the plasma. Although there might be an uncertainty in the absolute value of the ELM energy loss from the plasma (which is derived from a scaling, see [1] for details), the relative behaviour is important.

A direct measurment of the energy loss from the plasma due to small type-III ELMs is difficult. However, a simple estimation of the energy loss on the basis of a power balance will give more confidence. In steady state the ELM energy loss is determined by the inter-ELM energy transport and the ELM frequency (for type-III ELMs). The inter-ELM transport leads usually to a radiative power fraction (base line) of $f_{\text{rad}}^{\text{bl}} = 30 - 40\%$ (see also [1]), whereas the convective inter-ELM energy to the target is in the order of $f_{\text{W share}} = 50 - 100\%$ of the convected ELM energy to the target. Furthermore only a fraction of the energy lost at the pedestal during an ELM arrives at the target plates $f_{\text{target}} = 50 - 60\%$. For those highly radiating type-III ELMy H-modes complete detachment inbetween ELMs is observed and hence no inter-ELM power flux to the target is present. Altogether the energy loss by an ELM can be estimated on the basis of the above mentioned assumptions:

$\Delta W_{\text{ELM}} = [P_{\text{in}}(1-f_{\text{rad}}^{\text{bl}}) f_{\text{W share}}] / [f_{\text{ELM}} (f_{\text{target}} + f_{\text{W share}})]$. For the Pulse No: 53318 shown in fig.1 the maximum and minimum estimate of ΔW_{ELM} is 17kJ respectively. However, the total radiative of $f_{\text{rad}} \approx 90\%$ (Pulse No: 90%) is only consistent with the lower estimation of $\Delta W_{\text{ELM}} = 10\text{kJ}$.

Although the heat load can be reduced significantly, the confinement of these discharges is reduced as well. However, increasing the triangularity from $\delta = 0.2$ to $\delta = 0.47$ leads to improved confinement at high densities generally.

Figure 2 shows the dependence of the $H_{98(Y,2)}$ for radiative type-III ELMy H-modes with radiative power fractions of 70% and larger as function of the plasma density. As observed in the unseeded discharges reasonable confinement $H_{98(Y,2)} \approx 0.75$ can be kept up to densities close to the Greenwald density $\bar{n}_e/n_e^{\text{GW}} = f_{\text{GDL}} = 1$. For low densities high Z_{eff} are observed. An increase in absolute density ($Z_{\text{eff}} \propto P_{\text{rad}}/n_e^2$) leads to a reduction of the plasma core impurity content. The lowest $Z_{\text{eff}} (\approx 1.6)$ was achieved in high triangularity 2.5 MA / 2.7T pulses. No impurity accumulation has been observed. The profile of the fully ionised nitrogen, as derived from CXRS, is hollow during the highest radiative power fractions.

This radiating type-III ELMy H-mode might enable an integrated ITER scenario for $Q = 10$ operation with acceptable steady state and transient target power loads. For a slightly degraded confinement ($H_{98(Y,2)} = 0.75 - 0.8$) a $Q = 10$ operation will be possible at a plasma current of 17MA ($\beta_N \approx 1.5$, $f_{\text{GDL}}^{\text{GDL}} = 1$, $q_{95} = 2.6$) [2, 3]. This operational domain for 17MA is shown in figure 3.

Though operation at low “ might be difficult due to MHD, the operational domain at low tri-

angularity and high radiative power fractions ($f_{\text{rad}} \geq 0.7$) has been extended to low $q_{95} = 2.6$ with no apparent drawback due to MHD. The confinement ($H_{98(Y,2)} = 0.75$) is just acceptable even at lowest edge safety factors (see figure 4 for the best pulses. Some reduction of the confinement at low edge safety factors is observed. The reason for this is still under investigation.

3. RADIATIVE TYPE-I ELMY H-MODES

As alternative to the nitrogen seeded discharges, argon is seeded in type-I ELMy H-modes in order to reduce the transient heat flux due to larger ELMs (energy losses due to ELMs of $\Delta W_{\text{ELM}} \geq 0.2\text{MJ}$) since it has the potential to radiate at higher temperatures. In this scenario a confinement of $H_{98(Y,2)} = 1$ can be maintained at densities of $f_{\text{GDL}} \geq 0.85$, up to radiative power fractions of 65%, provided an accurate adjustment of both the Argon and Deuterium fuelling rates [4].

In the series of experiments reported here, emphasis has been given to the analysis of the ELM heat flux in discharges, which have not been performance optimised ($H_{98(Y,2)} \approx 0.87$, $f_{\text{GDL}} = 0.78$ which is 5% less than in Deuterium Reference pulse, and $f_{\text{rad}} = 0.6$): detailed measurements of the pedestal parameters (edge LIDAR and ECE data) and of the power fluxes to the target plates (IR camera) have been obtained. In these experiments, the frequency of the type-I ELMs decreases slightly as the power crossing the pedestal is decreasing (due to enhanced radiative power from the plasma core), and the transient divertor power load is reduced by a factor of ≈ 2 (figure 5). The resulting peak value at the outer divertor target is $\approx 15\text{MW/m}^2$, i.e. a factor of 3 higher when compared to the type-III ELMy H-mode with similar heating power. This reduced transient heat flux with Argon seeding stems from a reduced pedestal electron temperature (figure 6). This is furthermore illustrated in figure 7, which shows the energy rise at the divertor target versus the loss of stored plasma energy: no difference between data from Argon seeded and non-seeded discharges is observed, demonstrating the lack of additional dissipation in the SOL and divertor plasma under the present conditions. However, for similar ELM losses $\Delta W_{\text{ELM}}/W_{\text{ped}}$ Argon seeded discharges have a lower ELM frequency (by up to a factor of two lower, see figure 8), which is beneficial for the divertor lifetime.

Argon seeding in type-I ELMy H-modes would enable an integrated ITER scenario for $Q = 10$ operation at 15MA ($q_{95} = 3$). Confinement and density are well within the ITER requirements [5]. However, the aimed radiative power fraction of $f_{\text{rad}} = 0.75$ is difficult to reach in this scenario. This is consistent with the observation that the steady state heat flux to the divertor is not significantly reduced in those pulses. The maximum radiative power fraction has to be limited in order to avoid accumulation of argon in the plasma center, although the application of central heating might enable high impurity concentrations without accumulation in the plasma core [6].

4. MODELLING

4.1. MODELLING OF RADIATIVE COOLING OF PEDESTAL BY MIST

Modelling of the effect of impurity seeding on the transient power load on the divertor tiles has been carried with MIST and EDGE2D. The calculations with MIST suggest that Krypton is the best

element for the reduction of the divertor power load. However, since high-Z elements radiate strongly in the plasma core the acceptable impurity concentration of those elements is less than for low-Z impurities.

4.2. MODELLING OF RADIATIVE DISSIPATION IN SOL BY EDGE2D

In order to investigate the effect of radiative dissipation in highly radiating plasmas, EDGE2D modelling has been carried out. As reference plasma the Pulse No:53318 was taken with the Mk-II Gas Box divertor as boundary. The total heating power is $\approx 11\text{MW}$ with 8MW input power to the modelling grid. Nitrogen is seeded in this discharge with a rate of 8×10^{21} atoms/s, which is comparable with the fuelling rate from the outer divertor achieving those high radiative power fractions. The radiative power fraction is 85%, with Nitrogen the main radiator (60% of the total radiated power is from Nitrogen and 40% from Carbon). This target plasma is used as a basis to study the influence of the ELM energy on the target energy load. The ELM is simulated by an increased radial diffusion coefficient. The initial diffusion coefficient profile, which has been chosen to reproduce realistic pedestal electron temperature profiles [7], is multiplied by a constant factor. Typically the diffusion coefficient is in the center $\approx 0.5\text{m}^2\text{s}^{-1}$ and in the SOL $\approx 1\text{m}^2\text{s}^{-1}$. Around the pedestal region the diffusion coefficient is reduced to negligible values (for details see [7]). Increasing the diffusion coefficient by factors of 2.5, 5, 10 and 30 did lead to ELM energies of 5, 10, 20 and 60kJ. The duration of the increased transport is 0.5s. An example of such an ELM simulation is shown in figure 9. Modelling of the ELM mitigation demonstrates that a significant part of the ELM energy can be dissipated by radiation for ELMs smaller than 20kJ only 10. Increasing the ELM energy to 60kJ diminishes the effect of radiative dissipation in those highly radiative plasmas to negligible values of $\approx 20\%$. The target energy load due to ELMs for the larger ELMs (60kJ) is about 50% of the ELM energy loss from the plasma consistent with experimental observations (see above). Without the cooling of extrinsic impurities (here Nitrogen) ELM mitigation of small ELMs (25kJ) is even less effective ($\leq 20\%$ gets dissipated).

As observed in the experiment the electron temperature in front of divertor targets does stay below 14eV (during the ELM peak) for ELM energies below 10kJ. For those small ELMs Nitrogen becomes the main radiator during the ELM heat flux, whereas for the larger ELMs ($\Delta W_{\text{ELM}} \geq 20\text{kJ}$) Carbon radiates stronger than Nitrogen. The increased target fluxes during the ELM event lead to an increased carbon release and then subsequently radiate part of the ELM energy.

Those EDGE2D modelling results are consistent with B2/Eirene simulations for ITER [8], which show that only very small ELMs can be dissipated by a radiating layer. A comparison of recycling impurities versus non-recycling impurities has been carried out (1% recycling versus 90% recycling), which showed essentially no significant difference in the effect of radiative dissipation.

5. DISCUSSION

In order to assess the applicability of both impurity seeding scenarios the expected ELM size in

ITER has to be estimated. Figure 12 shows the dependence of the ELM energy loss on the collisionality. Both, in type-I ELMy H-modes [10] and in type-III ELMy H-modes the ELM energy loss $\Delta W_{\text{ELM}}/W_{\text{ped}}$ increases with decreasing pedestal collisionality. Argon seeded type-I ELMy H-modes have the same ELM energy loss $\Delta W_{\text{ELM}}/W_{\text{ped}}$ as unseeded type-I ELMy h-modes for similar collisionalities. For type-III ELMy H-modes also no difference between impurity seeded and non-seeded discharges with respect to the ELM energy losses $\Delta W_{\text{ELM}}/W_{\text{ped}}$ is observed. One should note that the values of $\Delta W_{\text{ELM}}/W_{\text{ped}}$ used in Fig. 12b for type-III ELMs are upper boundary estimates of the real ELM losses, since the noise level in the magnetic measurements is comparable to ΔW_{ELM} . Even considering this upper boundary estimate, the energy loss in type-III ELMy H-modes is a factor of ≈ 2 lower than in type-I ELMy H-modes. The real ELM losses can be up to a factor of two lower than these estimates, as some kinetic measurements of ΔW_{ELM} indicate [1]. For ITER, an ELM size of $\Delta W/W_{\text{ped}}$ of $9 \pm 5\%$ (assuming $W_{\text{ped}} = 30\%W_{\text{dia}}$ seems to be just acceptable [9, 10]. As shown in figure 12a, the contribution of the pedestal stored energy to the total stored energy is generally lower for type-III ELMs than for type-I ELMs, remaining within the ITER reference of $W_{\text{ped}} = 30\%$ even at high stored energy (and triangularity, up to $\delta \approx 0.5$). As in figure 12b demonstrated the type-III ELM losses are within the ITER acceptance even for the lowest collisionality, whereas for the ITER edge collisionality too large type-I ELM losses are observed. However, if the ELM size in ITER is not determined by the edge collisionality but rather by the parallel transport times in the SOL, type-I ELMy H-modes might be just acceptable [10].

Furthermore radiating ELMy H-modes have the advantage of lowering the target temperature due to radiation cooling inbetween ELMs in steady state. This generally, for type-I and type-III ELMy H-modes, allows for higher transient heat flux densities since the temperature of carbon ablation (1800°C) limits the transient heat flux.

With respect to the ITER requirements the best discharge is shown in the six-fold diagramme. Pulse No: 55969 demonstrates the ability of the type-III ELMy H-mode to meet all requirements for an integrated ITER scenario.

CONCLUSION

By seeding impurities the steady state heat flux to the divertor target plates can be reduced significantly. Radiative power fractions of 90% did lead to steady state power fluxes of less than 1 MW/m^2 . For both type-III ELMy H-modes and type-I ELMy H-modes a reduction of the transient heat flux was observed. This reduction of the heat flux is mainly due to a decrease of the pedestal energy in the presence of impurity fuelling. In addition ELM mitigation by radiative dissipation of the ELM energy was observed for the smallest type-III ELMs. This radiative dissipation of ELM energy is not expected for ITER, since the ELM energy will be likely in excess of several MJ. Hence, the ELM energy loss has to be limited. It is expected that for ITER-like pedestal collisionalities type-III ELMs are acceptable, whereas type-I ELMs are not. However, if the ELM losses are not determined by the pedestal collisionality type-I ELMy H-mode might be acceptable [11].

ACKNOWLEDGEMENT

This work has been conducted under the European Fusion Development Agreement.

REFERENCES

- [1]. RAPP, J., et al., Plasma Phys. Control. Fusion 44 6, 639 (2002)
- [2]. SHIMADA, M., et al., J. Plasma Fusion Res. SERIES, 3 p77 (2000)
- [3]. CAMPBELL, D.J., Phys. Plasmas 8 2041 (2001)
- [4]. DUMORTIER, P., et al., Plasma Phys. Control. Fusion 44 9, 1845 (2002)
- [5]. ONGENA, J., et al., submitted to Nucl. Fusion
- [6]. NAVE, M.F.F., et al., submitted to Nucl. Fusion
- [7]. KALLENBACH, A., et al., Proc. 28th European Physical Society Conf. on Controlled Fusion and Plasma Physics (Montreux, Switzerland, June 2002) Europhys. Conf. Abstr. vol 26a
- [8]. LOARTE, A., et al., IAEA-CN-77 ITERP/11(R) • 28...;£¢ IAEA Conference (Sorrento, Italy, 4-10 October 2000) Fusion Energy 2000 (IAEA, Vienna, 2001)
- [9]. FEDERICI, G., et al., PSI 2002 (Gifu, Japan, May 2002)
- [10]. LOARTE, A., et al., PSI 2002 (Gifu, Japan, May 2002)
- [11]. LOARTE, A., et al., this conference

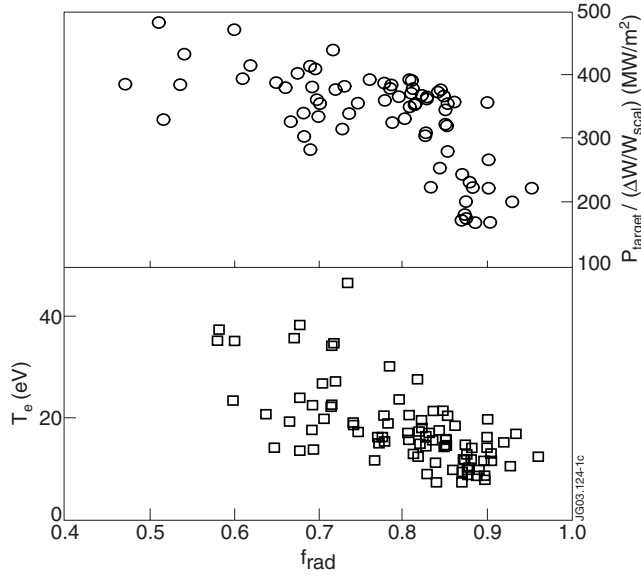


Figure 1: Pulse No: 53318, ratio of power density to the outer divertor target to the predicted $\Delta W/W$ -scaling and the electron temperature in front of the target during the ELM-peak, versus the radiative power fraction.

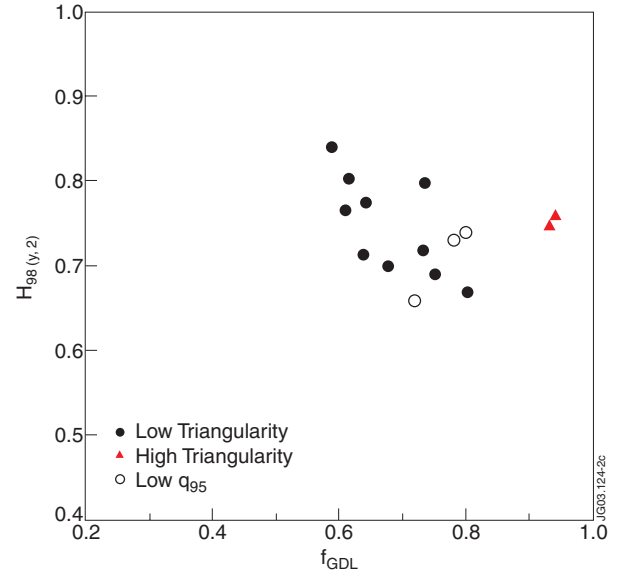


Figure 2: $H_{98(y,2)}$ versus the normalised density $\bar{n}_e/n_{GW} = f_{GDL}$, type-III ELMy H-modes with $f_{rad} \geq 0.7$.

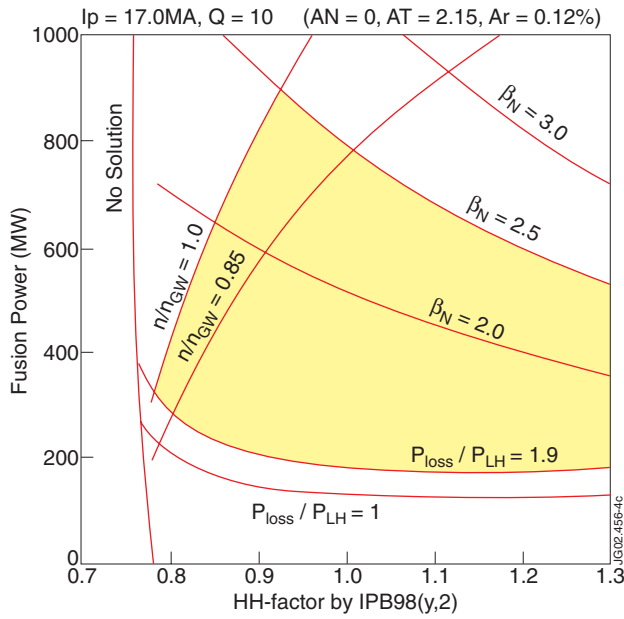


Figure 3: Fusion power versus the confinement enhancement factor $H_{98(y,2)}$, the $Q=10$ domain is indicated by the shaded area. (figure was given by courtesy of M. Shimada)

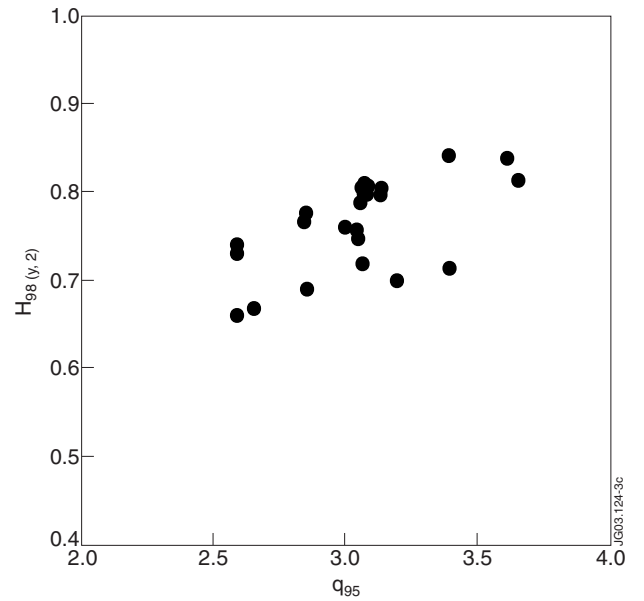


Figure 4: $H_{98(y,2)}$ versus the edge safety factor q_{95} , type-III ELMy H-modes with $f_{rad} \geq 0.7$.

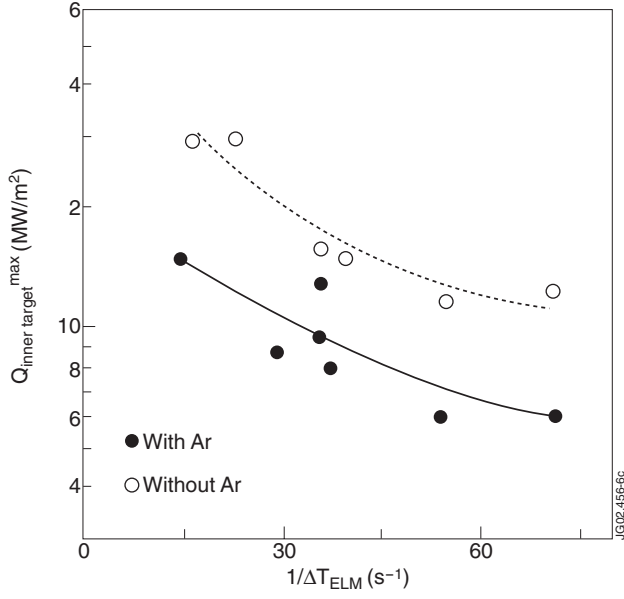


Figure 5: Comparison of power fluxes to the inner divertor target with ($f_{rad} \approx 0.6$) and without Argon fuelling.

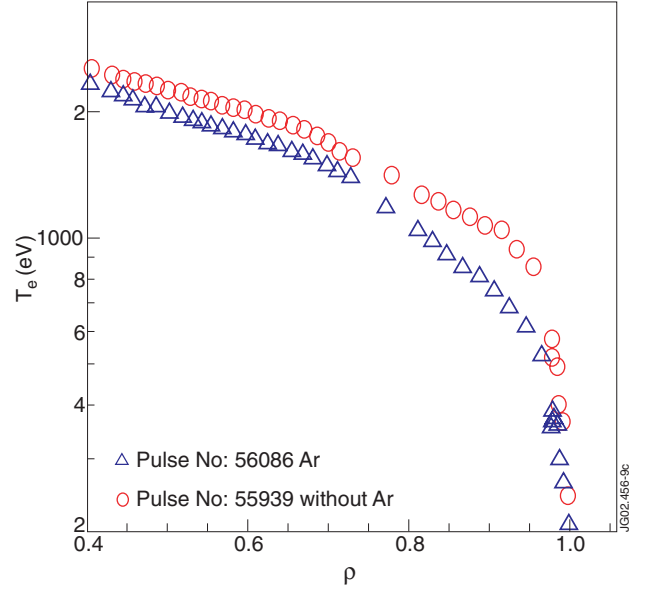


Figure 6: Comparison electron temperature profiles with and without Argon seeding.

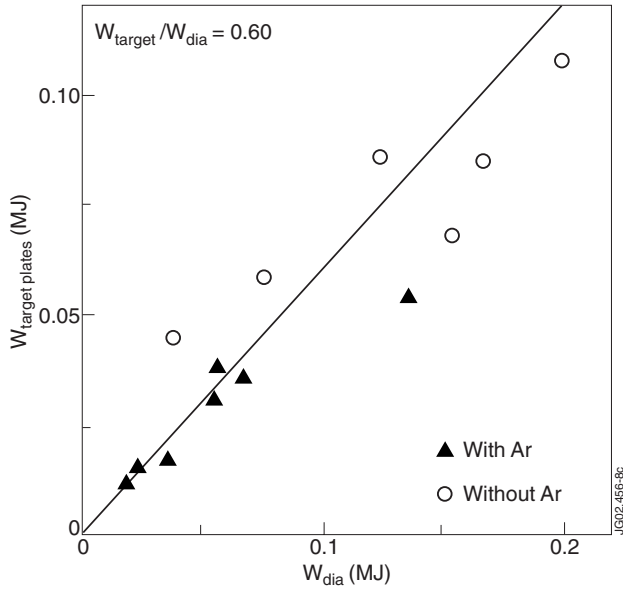


Figure 7: Reduction of target energy load due to ELMs versus energy lost from plasma due to ELMs.

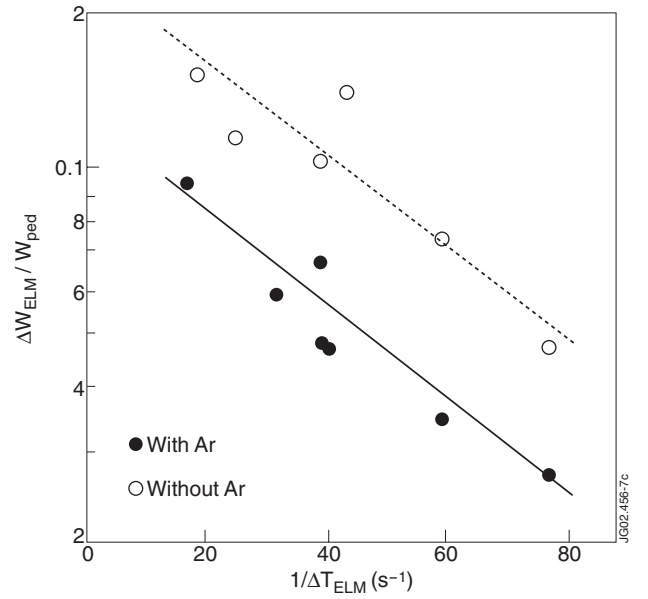


Figure 8: Dependence of ELM energy losses versus ELM frequency.

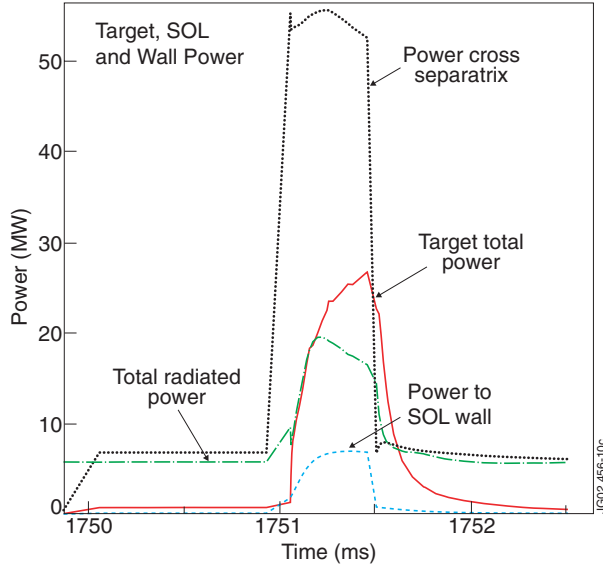


Figure 9: Example of an ELM simulation with EDGE2D: 25kJ ELM.

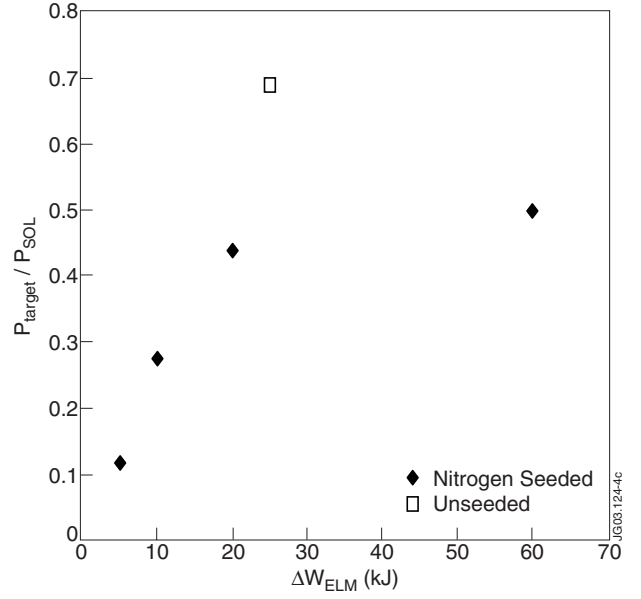


Figure 10: Ratio of target power load to power into the SOL during ELM event versus the ELM stored energy loss.

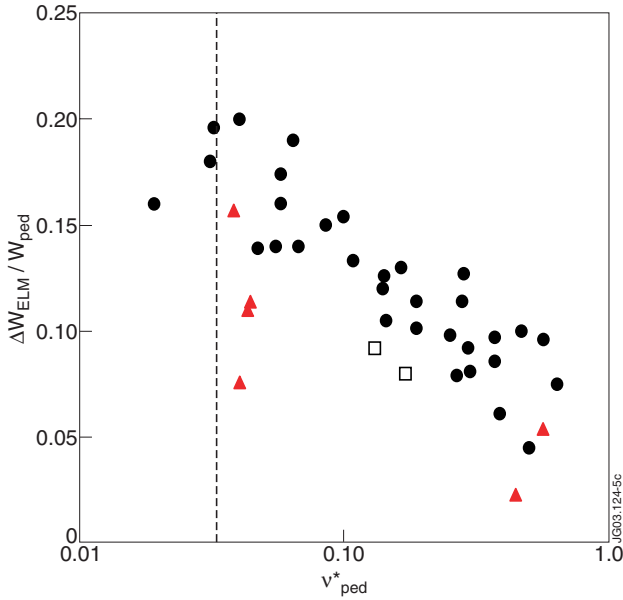


Figure 11: Comparison of type-III ELMy H-modes to type-I ELMy H-modes: plasma energy loss due to ELMs normalised to pedestal stored energy versus pedestal ion collisionality; non-seeded type-I ELMy H-modes (black solid circles), seeded type-I ELMy H-modes (black open squares), seeded and non-seeded type-III ELMy H-modes (red solid triangles); the ITER collisionality (dashed line).

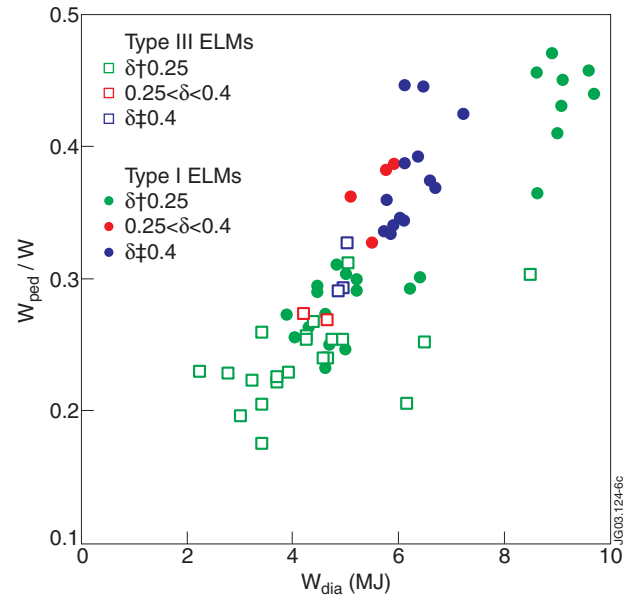


Figure 12: Comparison of type-III ELMy H-modes to type-I ELMy H-modes: Ratio of pedestal to total stored energy versus stored plasma energy.

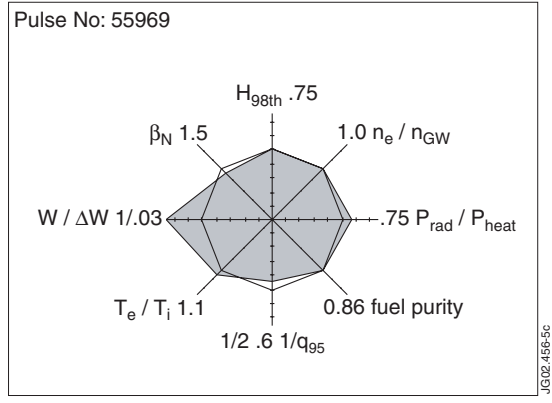


Figure 13: $H_{98(Y,2)}$ versus the normalised density \bar{n}_e/n_{GW}
 $= f_{GDL}$, type-III ELMy H-modes with $f_{rad} \geq 0.7$.